

Linear polarization of x rays emitted in radiative recombination into the *K* and *L* shells of Kr, Xe, Bi, and U ions

Tianluo Luo,^{1,*} Zhencen He^{2,1,*} Zhihao Yang³ Mingliang Duan,¹ Xianliang Liu,¹ Liangbo Xu,¹ Shuyu Zhang² Xiang Gao^{4,5,†} and Zhimin Hu^{1,‡}

¹Key Laboratory of Radiation Physics and Technology of Ministry of Education, Institute of Nuclear Science and Technology, Sichuan University, Chengdu 610064, China

²West China School of Basic Medical Sciences and Forensic Medicine, Sichuan University, Chengdu 610041, China

³College of Intelligent Manufacturing, Sichuan University of Arts and Science, Dazhou 635000, China

⁴Institute of Applied Physics and Computational Mathematics, Beijing 100088, China

⁵National Key Laboratory of Computational Physics, Beijing 100088, China



(Received 6 April 2023; revised 29 November 2023; accepted 10 January 2024; published 30 January 2024)

Recently, the polarization measurement of *L*-shell radiative recombination (*L*-RR) x rays was performed on the Tokyo-EBIT [N. Numadate *et al.*, *Phys. Rev. A* **105**, 023109 (2022)], and the reported theoretical result performed by the flexible atomic code (FAC) was higher than the experimental value. We present joint theoretical investigations on the linear polarization of x rays emitted from the RR into Kr, Xe, Bi, and U ions by two distinct theoretical approaches, i.e., the present relativistic calculations and the revised FAC using the density matrix formalism, in which the relativistic and multipole effects are fully considered. In addition, the energy and atomic number *Z* dependences of *L*-RR x-ray polarization are further investigated. Our results are in good agreement with experimental values for *K* shells and are closer to those for *L* shells than previous calculations. However, deviations still exist between the theoretical calculations and experimental results for *L* shells. It is found that the effect of the configuration interaction and the finite nuclear size on the polarization of *L*-RR x rays is not substantial. More theories and experiments are required to explain these deviations.

DOI: [10.1103/PhysRevA.109.012822](https://doi.org/10.1103/PhysRevA.109.012822)

I. INTRODUCTION

Radiative recombination (RR) is an electron-ion collision process in which the ion captures free electrons and emits photons simultaneously. This process plays an essential role in plasma research, such as astrophysical plasmas [1,2], vacuum spark plasmas [3–5], and laser-produced plasmas [6]. Furthermore, RR has attracted much attention since it is considered as a time-reversed process of photoionization [7–9]. Therefore, the studies on RR provide a novel approach to investigate the photoionization process.

In photoionization, the angular distribution of photoelectrons may exhibit anisotropy if the incident photons are polarized. Consequently, the RR x rays can be polarized if the incident electron beam is unidirectional. This feature has made the measurements of the angular distribution of emitted x rays widely used to study the relativistic effect in RR [8–12]. With the advent of Compton polarimetry [13], studies on x-ray polarization may become a more efficient way to investigate the relativistic effect in RR. Since then, experimental and theoretical studies of RR x-ray polarizations were extensively carried out [7,13–19]. Most recently, the polarization measurement of *L*-shell RR (*L*-RR) x rays from highly charged bismuth ions was performed by using the Electron Beam Ion Trap Compton Camera (EBIT-CC)

installed on the Tokyo-EBIT [20], and the calculated linear polarization 0.716 ± 0.023 performed by the flexible atomic code (FAC) was significantly higher than the experimental value, 0.666 ± 0.014 [21]. In addition, it was found that the measured *L*-RR x-ray polarization 0.41 ± 0.1 was overestimated by the FAC result 0.59 for the krypton measurement on the Free Electron Laser in Hamburg (FLASH)-EBIT [22]. Despite numerous reviews on RR, there is still a lack of detailed discussion regarding the linear polarization of *L*-RR. To date, the theoretical overestimation of the *L*-RR x-ray polarization remains unsolved.

In this paper, we present theoretical investigations on the linear polarization of x rays. Special attention is paid to *L*-RR. Due to the lack of high-energy polarization measurements, some previous theoretical investigations on multipole effects focused on a single multipole transition, e.g., the theoretical basis for the old FAC polarization module [18]. Therefore, there was little chance then to check the phase consistency among different multipole components, which turned out to be crucial for high-energy x-ray photons. To ensure the reliability of the theoretical polarization calculation, we carry out a joint theoretical calculation by two distinct theoretical methods, i.e., the present relativistic calculations and the revised FAC using the density matrix formalism. We calculate the polarizations of *K*-RR and *L*-RR x rays into Kr, Xe, Bi, and U ions at different energies. The excellent agreement between these two calculations clearly demonstrated their quantitative reliability. The energy and atomic number *Z* dependences of *L*-RR x-ray polarization are also investigated. Our results indicate that the energy and atomic number *Z* can cause a significant change in

*These authors contributed equally to this work.

†gao_xiang@iapcm.ac.cn

‡huzhimin@scu.edu.cn

the polarization of x rays emitted from the RR into different magnetic sublevels of L shells. Compared to those of $2s_{1/2}$ and $2p_{1/2}$ shells, the linear polarization of RR for the electron captured in the $2p_{3/2}$ shells is more sensitive to the change in electron energy. The calculations are compared with the theoretical results using the old FAC and the previously reported experimental measurements. The comparison shows that our calculations are in good agreement with experimental values for K -RR and are closer to those of L -RR than previous calculations. However, deviations still exist between the theoretical calculation and experimental results. It is found that the effect of the configuration interaction and the finite nuclear size on the polarization of L -RR x rays is not the main reason for these deviations.

II. THEORY

A. The theoretical framework of RR x-ray polarization

In this work, the method is in a framework similar to that of Eichler *et al.* [14]. It is assumed that an electron of a bound state with a Dirac quantum number κ_n and angular momentum projection μ_n is expressed as $|\kappa_n \mu_n\rangle$.

In photoionization, the bound electron transforms to a continuum free state with asymptotic momentum p and the electron spin projection $m_s = \pm \frac{1}{2}$, and this state can be expressed as $|pm_s\rangle$. We assume that the photon has helicity $\lambda = \pm 1$. Hence, the transform matrix element can be written as

$$M = \langle pm_s | \boldsymbol{\alpha} \cdot \hat{u}_\lambda \exp(ik \cdot r) | \kappa_n \mu_n \rangle. \quad (1)$$

Here, $\boldsymbol{\alpha}$ is the Dirac matrix, and \hat{u} is the unit vector of the polarized photon. The radiation field can be expressed as

$$\hat{u}_\lambda \exp(ik \cdot r) = \sqrt{2\pi} \sum_{L,M} i^L \sqrt{2L+1} (A_{LM}^m + i\lambda A_{LM}^e) D_{M\lambda}^L, \quad (2)$$

$$A_{LM}^m = j_L(kr) T_{LL}^M, \quad (3)$$

$$A_{LM}^e = j_{L-1}(kr) \sqrt{\frac{L+1}{2L+1}} T_{L,L-1}^M - j_{L+1}(kr) \sqrt{\frac{L}{2L+1}} T_{L,L+1}^M, \quad (4)$$

where the $D_{M\lambda}^L$ is the Wigner D function to convert the photon direction as the quantization axis to the electron direction. Then we can write the cross section of circularly polarized radiation as [16]

$$\begin{aligned} \sigma_\pm(\theta) &= 2\pi \mathcal{N} \sum_{\mu_n m_s} \sum_{\lambda=\pm 1} \sum_{\bar{L}} (-1)^{M+1} i^{L-\bar{L}} \\ &\times \sqrt{(2L+1)(2\bar{L}+1)} \sum_v \begin{pmatrix} L & \bar{L} & v \\ M & -M & 0 \end{pmatrix} \\ &\times \begin{pmatrix} L & \bar{L} & v \\ \lambda & -\lambda & 0 \end{pmatrix} \\ &\times \langle pm_s | \boldsymbol{\alpha} \cdot A_{LM}^\lambda | \kappa_n \mu_n \rangle \langle pm_s | \boldsymbol{\alpha} \cdot A_{LM}^\lambda | \kappa_n \mu_n \rangle^* \\ &\times P_v(\cos \theta), \end{aligned} \quad (5)$$

$$\mathcal{N} = \frac{\alpha^3 \hbar^2 \omega^2 a_0^2}{8m_e(\alpha^2 \epsilon^2 + 2\epsilon)}, \quad (6)$$

where $M = m_s - \mu_n$ and $A_{LM}^\lambda = A_{LM}^m + i\lambda A_{LM}^e$, θ is the observation angle, P_v is the Legendre polynomials [23], α is the fine structure constant, a_0 is the Bohr radius, ω is the photon energy, and ϵ is the electron energy. Here, we can expand the Dirac continuum wave function of the electron into partial waves $|\kappa m_s\rangle$, and the transition matrix elements $\langle pm_s | \boldsymbol{\alpha} \cdot A_{LM}^\lambda | \kappa_n \mu_n \rangle$ can be expressed as

$$\begin{aligned} \langle pm_s | \boldsymbol{\alpha} \cdot A_{LM}^\lambda | \kappa_n \mu_n \rangle &= \sum_\kappa i^{-l} e^{i\Delta_\kappa} \sqrt{4\pi(2l+1)} \\ &\times \begin{pmatrix} l & \frac{1}{2} & j \\ 0 & m_s & m_s \end{pmatrix} \\ &\times \langle \kappa m_s | \boldsymbol{\alpha} \cdot A_{LM}^{(\lambda)} | \kappa_n \mu_n \rangle, \end{aligned} \quad (7)$$

where Δ_κ is the Coulomb phase shift. Depending on different atomic systems in our investigations, the Dirac atomic orbitals are generated from either a pure Coulomb potential or a Dirac-Slater self-consistent potential. If the Dirac-Slater self-consistent field is used in the calculation, then the short-range phase shift should also be included in Δ_κ . The last item in the above formula is the general multipole matrix element, where the calculation formula can be found in Ref. [24].

To calculate the cross section for the photon in the direction of polarization σ_ϕ in the reaction plane, one should take the interference terms σ_ϕ^{int} between the helicity of circular polarization $\lambda = \pm 1$ into account, where ϕ is the azimuth angle of the polarization direction of the photon relative to the direction of the electron being injected. Therefore, the cross section of linear polarization can be expressed

$$\sigma_\phi(\theta) = \sigma_0(\theta) + \sigma_\phi^{\text{int}}(\theta), \quad (8)$$

where σ_0 is the cross section averaged over photon polarizations, and is equal to σ_\pm . The interference terms can be written as

$$\begin{aligned} \sigma_\phi^{\text{int}}(\theta) &= \pi \mathcal{N} \sum_{\mu_n m_s} \sum_{\lambda=\pm 1} \sum_{\bar{L}} (-1)^{M+1} i^{L-\bar{L}} e^{i2\lambda\phi} \\ &\times \sqrt{(2L+1)(2\bar{L}+1)} \sum_v \begin{pmatrix} L & \bar{L} & v \\ M & -M & 0 \end{pmatrix} \\ &\times \begin{pmatrix} L & \bar{L} & v \\ \lambda & \lambda & 2\lambda \end{pmatrix} \langle pm_s | \boldsymbol{\alpha} \cdot A_{LM}^\lambda | \kappa_n \mu_n \rangle \\ &\times \langle pm_s | \boldsymbol{\alpha} \cdot A_{LM}^{-\lambda} | \kappa_n \mu_n \rangle^* \sqrt{\frac{(v-2)!}{(v+2)!}} P_v^2(\cos \theta), \end{aligned} \quad (9)$$

where P_v^2 is the associated Legendre polynomials. The degree of linear polarization can be written as

$$P = \frac{1 - \sigma_\perp/\sigma_\parallel}{1 + \sigma_\perp/\sigma_\parallel} = \frac{\sigma_\parallel^{\text{int}}}{\sigma_0}, \quad (10)$$

where $\sigma_\perp = \sigma_{\phi=\pi/2}$ is the cross section for photons polarized in the direction perpendicular to the reaction plane, and $\sigma_\parallel = \sigma_{\phi=0}$ is parallel to the reaction plane. The relationship between different emitted angles and directions can be found in Fig. 1.

To facilitate the calculation of the RR angular distribution and the linear polarization using the FAC, one can simplify

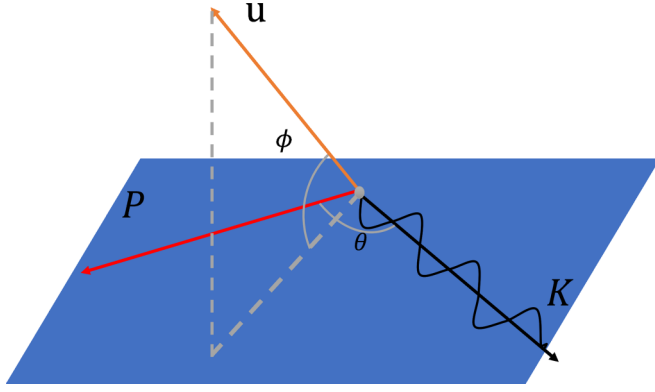


FIG. 1. The relationship between different emitted angles and directions. It is assumed that the direction of photon K and electron P are located on the reaction plane. The angle between K and P is θ , and the angle between the unit vector u of the linear polarization, which is perpendicular to K , and the reaction plane is ϕ .

the formula from Eqs. (5) and (9) as [18]

$$\sigma_{\text{FAC}}^{\text{RR}}(\theta) = \frac{\sigma_{\text{FAC}}^{\text{RRT}}}{4\pi} \left[\sum_{\nu \geq 0} B_{\nu} P_{\nu}(\cos \theta) - \sum_{\nu \geq 2} \nu^{-1} (\nu - 1)^{-1} B_{\nu}^{\phi} P_{\nu}^2(\cos \theta) \cos(2\phi) \right], \quad (11)$$

where $\sigma_{\text{FAC}}^{\text{RRT}}$ is the total RR cross section, B_{ν} and B_{ν}^{ϕ} are calculated using the ASYMMETRY function based on the density matrix formalism. For the dipole transition, $\nu = 2$ and B_{ν} is equal to B_{ν}^{ϕ} , while for the quadrupole transition, $\nu = 4, \dots$, and so on. Equation (11) offers greater convenience for considering the electron correlation in further analysis.

B. Two different calculation programs

In this work, we use two different calculation programs for computing the matrix elements and polarization parameters, i.e., the present relativistic calculations and the FAC using the density matrix formalism.

In the present relativistic calculations, summing and averaging over the unobserved variables are performed explicitly, and the central field is established as a pure Coulomb potential. Compared with the present relativistic calculations, the FAC using density matrix formalism provides a systematic and elegant basis for summing and averaging the unobserved variables, which can avoid the introduction of unnecessary variables and expedite the calculations [7,25–27]. To calculate the polarization of photons emitted from the RR by using the FAC, the ASYMMETRY function is used to calculate the radiative transition process from bound states to free states [28].

In an earlier version (earlier than December 2022) of the FAC (labeled as OFAC), almost all calculations produce higher polarizations than the experiments because of an incorrect use of the phase factor. Due to the lack of high-energy polarization measurements, OFAC just focused on a single multipole transition, and it only works when the electric dipole ($E1$) approximation dominates. The latest version of

TABLE I. The experimental linear polarization of K -RR into bare Kr, Xe, and U ions, as well as the calculation results by using the present relativistic calculations and NFAC at corresponding incident electron energies and observation angles.

Z	θ (deg)	Energy (keV)	Present (%)	NFAC (%)	Expt. ^a (%)
36	90	58	98.19	98.19	96.2 ± 2.3
54	105	16.9	98.98	98.98	99.9 ± 1.5
	122	81.7	96.69	96.69	95.6 ± 1.7
92	85	53.4	86.07	86.07	85 ± 7
	89	71.9	84.00	84.02	83 ± 5
	95	103.5	80.57	80.60	72 ± 5
	110	217.9	69.74	69.75	61 ± 12
	136	217.9	83.73	83.74	79 ± 8

^aThe experimental results are taken from Refs. [13,20,29].

the FAC (labeled as NFAC) solves this problem and gives more reasonable results, such as the RR differential cross section and the polarization.

III. RESULTS AND DISCUSSION

To ensure the reliability of the calculation results, the linear polarizations of K -RR x rays into bare Kr, Xe, and U ions are calculated at incident electron energies of 58, 81.7, and 217.9 keV, respectively, using the present relativistic calculations and NFAC to compare with the experimental values. The calculations are carried out in the laboratory frame, which corresponds to the EBIT measurements. The strictly relativistic effects and a complete multipole expansion of the radiative field are fully considered in the calculations. Comparisons with other theoretical and experimental results are listed in Table I, which reveals that our calculation results are in good agreement with the experimental values for K shells.

Figure 2 shows the linear polarization as a function of emission angle θ for L -RR x rays into U ions at different electron energies. When an electron is captured in different magnetic sublevels, it will produce x rays with different polarization behaviors, so we need to calculate separately for the $2s_{1/2}$ ($L1$), $2p_{1/2}$ ($L2$), and $2p_{3/2}$ ($L3$) shells. A “crossover” feature is found in Fig. 2. For $L2$ shells, the linear polarization obtains a crossover feature at about 120 keV. Beyond this energy, linear polarization becomes increasingly negative at forward angles. Additionally, the energy required is approximately 150 keV for the crossover in $L3$ shells, while for $L1$ shells, it requires exceeding 230 keV. Moreover, the crossover angles for $L2$ and $L3$ are approximately 45° and 60° , respectively. Similar crossover features have been reported for the linear polarization of K -RR x rays into bare ions and the corresponding photoionization processes [14,30]. Figure 3 shows the linear polarization of L -RR x rays at 90° for atomic numbers Z from 35 to 92. In this calculation, three energies of two, four, and six times the ionization threshold of the first electron in the L shell are investigated. The present relativistic calculation and NFAC results show that the depolarization of the L -RR x rays with an increase of electron energy is particularly significant, and the linear polarization of $L3$ -RR is more sensitive to energy changes compared to those of

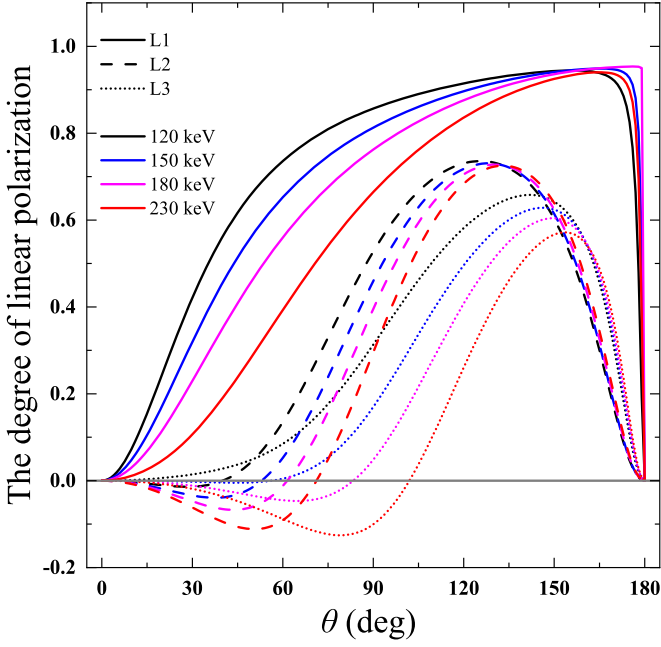


FIG. 2. Linear polarization of L -RR x rays into U ions. The results are given successively for the electron energies 120, 150, 180, and 230 keV, respectively. $L1$ (solid line), $L2$ (dashed line), and $L3$ (dotted line) represent the electron captured in the $2s_{1/2}$, $2p_{1/2}$, and $2p_{3/2}$ shells, respectively.

$L1$ -RR and $L2$ -RR as shown in Fig. 2. When the energy and atomic number Z are kept constant, the linear polarization of the different magnetic sublevels in the 90° direction is $L3 < L2 < L1$. In addition, the results of the three theoretical methods are close at lower energies for lower Z ions. As the energy increases, the OFAC results are obviously higher than the present relativistic and NFAC results, and such differences increase with energy. This shows the overestimation of the OFAC calculations. Note that the linear polarization of $L2$ does not exhibit a significant Z dependence as the other two magnetic sublevels. Here, the multipole convergence of the linear polarization is limited in the direction of an observation angle of 90° . To achieve the convergence of the calculated linear polarization of L -RR x rays into bare U ions, the multipoles need to reach 20, 36, and 36 for $L1$ -RR, $L2$ -RR, and $L3$ -RR at 230 keV, respectively, while the corresponding values are 16, 24, and 22 in turn at 120 keV.

Since the L -RR x-ray linear polarization includes different charge states and magnetic sublevels, the effective L -RR x-ray polarization is determined by averaging the polarizations for each orbital of every charge state, where the ion abundances and theoretical differential cross sections are taken into account as weights, and it can be expressed as

$$P = \frac{\sum_i P_i A_i \sigma_{0i}(90^\circ)}{\sum_i A_i \sigma_{0i}(90^\circ)}, \quad (12)$$

where P_i , A_i , and σ_{0i} are the linear polarization, ion abundance, and RR differential cross section of the charge state i , respectively. Here, the ion abundances A_i of Bi and Kr ions are derived from Refs. [21,22].

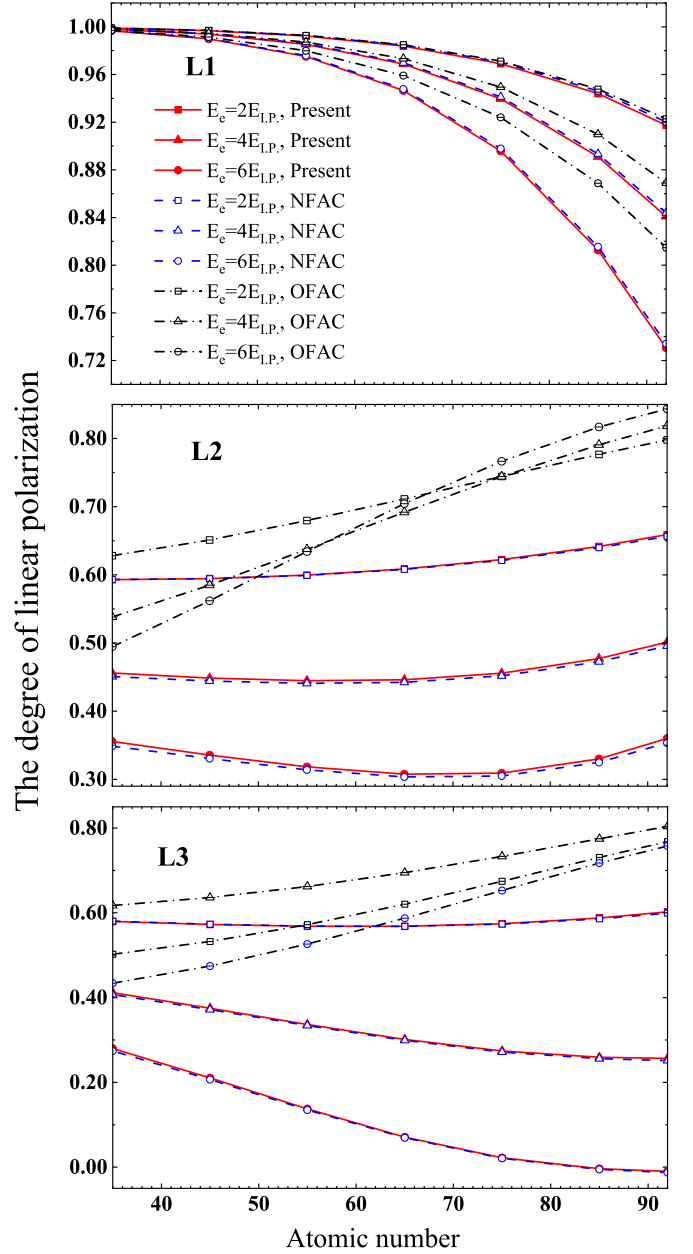


FIG. 3. The atomic number dependence of linear polarization of L -RR x rays with three theoretical methods at 90° . E_e and $E_{L,P}$ are the electron energy and ionization threshold of the first electron in the L shell, respectively.

Since the earlier version of FAC cannot correctly consider multipole transitions, the calculation result (0.716 ± 0.023) only took the $E1$ transition into account and it was compared with the experimental result (0.666 ± 0.014) measured on the Tokyo-EBIT [21]. The NFAC result is 0.627 ± 0.020 for L -RR x rays into Bi ions at 51.1 keV, and it is closer to the experiment than the previous calculation result. Furthermore, for L -RR x rays into Kr ions at 8.76 keV, the NFAC result is 0.57, which is also closer to the experimental value 0.41 ± 0.1 [22] than the previous calculation result (0.59). Here, the theoretical results for each ion are based on a single-state approximation as listed in the second column of Table II.

TABLE II. Configurations used in the NFAC calculations. N_{ele} stands for the number of electrons. C_i represents the configuration interaction coefficients. The figures in parentheses indicate powers of ten. For near-closed-shell ions such as F-like ions, the presence of a multiconfiguration is negligible.

N_{ele}	Config.	$ C_1 _{\text{Bi}}^2$	$ C_1 _{\text{Kr}}^2$	Config.	$ C_2 _{\text{Bi}}^2$	$ C_2 _{\text{Kr}}^2$	Config	$ C_3 _{\text{Bi}}^2$	$ C_3 _{\text{Kr}}^2$	$2J$
He-like	$1s^2$	1.00	1.00	$1s2s$	1.53(-2)	1.97(-2)	$2s^2$	3.34(-4)	1.40(-2)	0
Li-like	$1s^22s$	1.00	1.00	$1s2s^2$	5.10(-7)	1.66(-6)	$2s2p_{1/2}^2$	3.30(-7)	8.88(-7)	1
Be-like	$1s^22s^2$	0.98	0.97	$1s^22p_{1/2}^2$	1.53(-2)	1.97(-2)	$1s^22p_{3/2}^2$	3.42(-4)	1.40(-2)	0
B-like	$1s^22s^22p_{1/2}$	1.00	0.99	$1s^22p_{1/2}2p_{3/2}^2$	3.76(-4)	1.33(-2)	$1s2s2p_{1/2}2p_{3/2}^2$	4.51(-7)	2.86(-6)	1
C-like	$1s^22s^22p_{1/2}^2$	1.00	0.97	$1s^22p_{1/2}^22p_{3/2}^2$	3.59(-4)	2.29(-2)	$1s^22s^22p_{3/2}^2$	1.25(-4)	8.28(-3)	0
N-like	$1s^22s^22p_{1/2}^22p_{3/2}$	1.00	0.91	$1s^22p_{1/2}^22p_{3/2}^2$	1.77(-4)	6.85(-2)	$1s^22s^22p_{1/2}2p_{3/2}^2$	1.24(-4)	1.98(-2)	3
O-like	$1s^22s^22p_{1/2}^22p_{3/2}^2$	1.00	0.95	$1s^22p_{1/2}^22p_{3/2}^4$	3.48(-4)	4.05(-2)	$1s^22s^22p_{3/2}^4$	1.33(-4)	5.74(-3)	0
F-like	$1s^22s^22p_{1/2}^22p_{3/2}^3$									3

The uncertainty of the theoretical calculation of Bi ions is 1σ statistical error obtained from abundance fitting [21]. Since Ref. [22] does not mention the uncertainty in abundance fitting, the effective polarization calculations of Kr ions do not take the uncertainty into account.

There may be differences in the self-consistent potential and the magnitude of the electron correlation among different configurations. Hence, we employed the configuration interaction to account for electron correlations. The configurations used in the NFAC calculations are listed in Table II. For each ion species, we have only listed the three most significant contributing configurations. For near-closed-shell ions, e.g., F-like ions, the presence of a multiconfiguration is negligible. Figure 4 shows the configuration interaction coefficients of He-like to O-like ions as a function of atomic number. It is evident that, with the exception of Be-like ions (indicated by the purple dashed line), the configuration mixing approaches zero for high- Z ions. Therefore, it is interesting to see the configuration interactions for Be-like ions and lower- Z ions. For Be-like ions, the contribution of the configuration interaction to $L2$ polarization is almost neglected because the configuration state $1s^22p_{1/2}^2$ can no longer capture an electron

in the $2p_{1/2}$ orbital. In addition, for both the configurations $1s^22s^2$ and $1s^22p_{1/2}^2$, the captured $2p_{3/2}$ electron experiences almost a pure Coulomb potential of $Z - 4$ in high- Z ions. Therefore, the contribution of the configuration interaction to $L3$ polarization is almost negligible as well. For lower- Z ions, although the configuration mixing is significant, its contribution to the effective polarization is relatively small. The contributions of the configuration interaction to the effective polarization of L -RR x rays are 0.1% and 0.4% for Bi ions and Kr ions, respectively. Detailed calculation results can be found in Fig. 5. It is obvious that the contribution of the configuration interaction to the effective polarization of L -RR x rays is negligible. Reference [21] suggested that electron correlation was important for the polarization of the recombination x rays. However, our investigation demonstrates that, within this system, the effect of electron correlation is negligible, and the present NFAC results are closer to the experimental results than previous calculation results. In addition, we also consider the effect of finite nuclear size using Fermi distribution function models [31]. It can affect the wave functions of $1s$ and $2s$ orbitals in the nuclear region. However, the contribution of the finite nuclear size effect is less than 0.1% for the $L1$ -RR x-ray polarization into Bi ions at 51.1 keV. These factors explain that the effects of the configuration interaction and finite nuclear size are much smaller than the uncertainty of ion abundance. It is worth noting that the uncertainty of ion abundance in Ref. [21] is just a 1σ statistical error, and further attention is required to additional factors that may affect the uncertainty of ion abundance.

IV. SUMMARY

In summary, we theoretically investigate the linear polarization of x-ray photons emitted from the radiative recombination (RR) into K and L shells of Kr, Xe, Bi, and U ions by two distinct theoretical methods, i.e., the present relativistic calculations and the revised FAC using the density matrix formalism. Special attention is paid to L -RR. The energy and atomic number Z dependences of L -RR x-ray polarization are further investigated. It shows that the present results are in good agreement with the existing experiments for K -RR and are closer to those of L -RR than previous FAC calculations. However, deviations still exist between the theoretical calculations and experimental results. From the

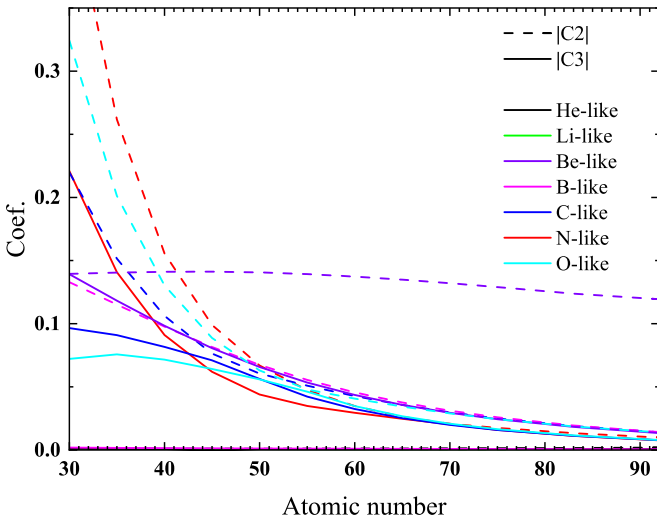


FIG. 4. Configuration interaction coefficients of He-like to O-like ions as a function of atomic number.

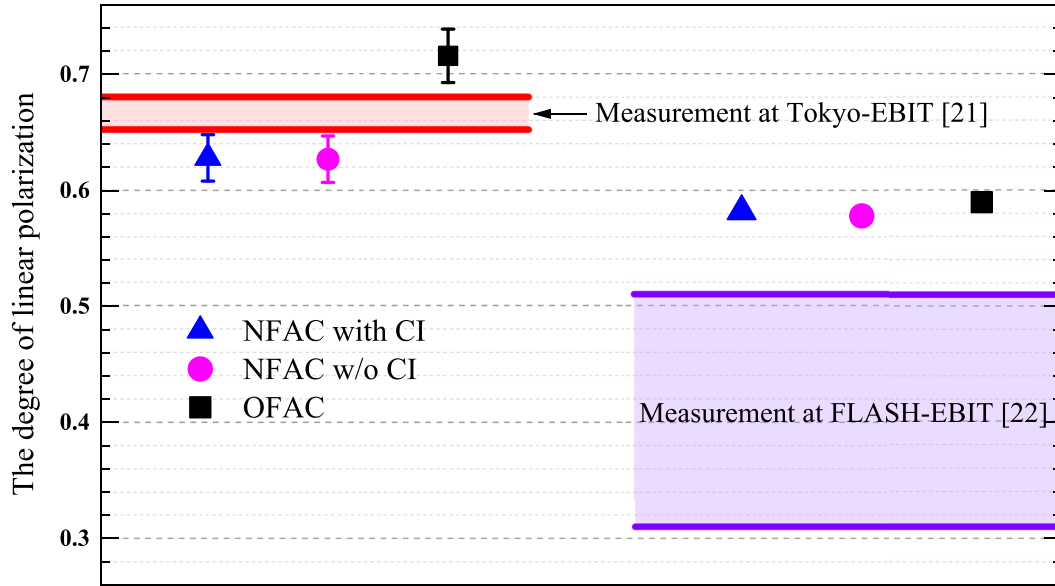


FIG. 5. Measurements (Bi ions at 51.1 keV [21] and Kr ions at 8.76 keV [22]) and theoretical calculations of L -RR x-ray linear polarizations. The blue triangles and pink circles represent the calculations of NFAC with and without the configuration interaction (CI), respectively. The black squares represent the calculations of the OFAC which are reported in previous papers.

results, the effect of the configuration interaction and the finite nuclear size on L -RR x-ray polarization is not important. Moreover, we found the uncertainty in ion abundance is important for this discrepancy. For Bi ions, by considering the 1σ statistical error of abundance fitting only, our calculated results almost reproduce the experiment within the uncertainties. Due to the lack of experimental uncertainty, we do not carry out the estimation for Kr ions. More theoretical and experimental works are required to improve the remaining deviations.

ACKNOWLEDGMENTS

We thank Dr. M. F. Gu for useful discussions and fixing the bugs in FAC via private communications. This work was supported by the National Key R&D Program of China (Grant No. 2022YFA1602500), the Sichuan Science and Technology Program (Grant No. 2023ZYD0017), the National Natural Science Foundation of China (Grants No. 12074352, No. 12374234, No. 12241410, No. 11774023, and No. 12304275), and the Fundamental Research Funds for the Central Universities in China (Grant No. YJ202144).

- [1] T. Tajima and K. Shibata, *Plasma Astrophysics* (CRC Press, Boca Raton, FL, 2002).
- [2] Z. Yang, Z. He, G. Xiong, K. Yao, Y. Yang, B. Wei, Y. Zou, Z. Wu, Z. Tian, Y. Ma, C. Wu, X. Gao, and Z. Hu, Apparent change of the 3C/3D line intensity ratio in neonlike ions, *Opt. Express* **30**, 25326 (2022).
- [3] C. R. Negus and N. J. Peacock, Local regions of high-pressure plasma in a vacuum spark, *J. Phys. D: Appl. Phys.* **12**, 91 (1979).
- [4] R. Beier, C. Bachmann, and R. Burhenn, Investigation of the polarisation of nonthermal bremsstrahlung from a vacuum spark plasma, *J. Phys. D: Appl. Phys.* **14**, 643 (1981).
- [5] P. Beiersdorfer, E. J. Clothiaux, and G. Bell, Axial magnetic field measurements and the stability of a vacuum spark plasma, *J. Phys. D: Appl. Phys.* **16**, 1635 (1983).
- [6] M. Mattioli and D. Véron, Electron-ion recombination in laser produced plasma, *Plasma Phys.* **11**, 684 (1969).
- [7] A. Surzhykov, S. Fritzsche, T. Stöhlker, and S. Tachenov, Polarization studies on the radiative recombination of highly charged bare ions, *Phys. Rev. A* **68**, 022710 (2003).
- [8] J. Eichler, A. Ichihara, and T. Shirai, Photon angular distributions from radiative electron capture in relativistic atomic collisions, *Phys. Rev. A* **51**, 3027 (1995).
- [9] T. Stöhlker, T. Ludziejewski, F. Bosch, R. W. Dunford, C. Kozhuharov, P. H. Mokler, H. F. Beyer, O. Brinzaescu, B. Franzke, J. Eichler, A. Griegal, S. Hagmann, A. Ichihara, A. Krämer, J. Lekki, D. Liesen, F. Nolden, H. Reich, P. Rymuza, Z. Stachura *et al.*, Angular distribution studies for the time-reversed photoionization process in hydrogenlike uranium: The identification of spin-flip transitions, *Phys. Rev. Lett.* **82**, 3232 (1999).
- [10] R. Anholt, S. A. Andriamonje, E. Morenzoni, C. Stoller, J. D. Molitoris, W. E. Meyerhof, H. Bowman, J.-S. Xu, Z.-Z. Xu, J. O. Rasmussen, and D. H. H. Hoffmann, Observation of radiative capture in relativistic heavy-ion-atom collisions, *Phys. Rev. Lett.* **53**, 234 (1984).
- [11] A. Ichihara, T. Shirai, and J. Eichler, Radiative electron capture in relativistic atomic collisions, *Phys. Rev. A* **49**, 1875 (1994).
- [12] T. Stöhlker, C. Kozhuharov, P. H. Mokler, A. Warczak, F. Bosch, H. Geissel, R. Moshhammer, C. Scheidenberger, J.

- Eichler, A. Ichihara, T. Shirai, Z. Stachura, and P. Rymuza, Radiative electron capture studied in relativistic heavy-ion-atom collisions, *Phys. Rev. A* **51**, 2098 (1995).
- [13] S. Tashenov, T. Stöhlker, D. Banaś, K. Beekert, P. Beller, H. F. Beyer, F. Bosch, S. Fritzsche, A. Gumberidze, S. Hagmann, C. Kozhuharov, T. Krings, D. Liesen, F. Nolden, D. Protic, D. Sierpowski, U. Spillmann, M. Steck, and A. Surzhykov, First measurement of the linear polarization of radiative electron capture transitions, *Phys. Rev. Lett.* **97**, 223202 (2006).
- [14] J. Eichler and A. Ichihara, Polarization of photons emitted in radiative electron capture by bare high-Z ions, *Phys. Rev. A* **65**, 052716 (2002).
- [15] J. H. Scofield, Angular and polarization correlations in photoionization and radiative recombination, *Phys. Rev. A* **40**, 3054 (1989).
- [16] J. Eichler, A. Ichihara, and T. Shirai, Alignment caused by photoionization and in radiative electron capture into excited states of hydrogenic high-Z ions, *Phys. Rev. A* **58**, 2128 (1998).
- [17] H. Jörg, Z. Hu, H. Bekker, M. A. Blessenohl, D. Hollain, S. Fritzsche, A. Surzhykov, J. R. Crespo López-Urrutia, and S. Tashenov, Linear polarization of x-ray transitions due to dielectronic recombination in highly charged ions, *Phys. Rev. A* **91**, 042705 (2015).
- [18] M. F. Gu, D. W. Savin, and P. Beiersdorfer, Effects of electron spiralling on the anisotropy and polarization of photon emission from an electron beam ion trap, *J. Phys. B: At. Mol. Opt. Phys.* **32**, 5371 (1999).
- [19] N. Nakamura, N. Numadate, S. Oishi, X.-M. Tong, X. Gao, D. Kato, H. Odaka, T. Takahashi, Y. Tsuzuki, Y. Uchida, H. Watanabe, S. Watanabe, and H. Yoneda, Strong polarization of a $J = 1/2$ to $1/2$ transition arising from unexpectedly large quantum interference, *Phys. Rev. Lett.* **130**, 113001 (2023).
- [20] Y. Tsuzuki, S. Watanabe, S. Oishi, N. Nakamura, N. Numadate, H. Odaka, Y. Uchida, H. Yoneda, and T. Takahashi, An application of a Si/CdTe Compton camera for the polarization measurement of hard x rays from highly charged heavy ions, *Rev. Sci. Instrum.* **92**, 063101 (2021).
- [21] N. Numadate, S. Oishi, H. Odaka, Priti, M. Sakurai, T. Takahashi, Y. Tsuzuki, Y. Uchida, H. Watanabe, S. Watanabe, H. Yoneda, and N. Nakamura, Polarization measurement of L-shell radiative recombination x rays from highly charged bismuth ions, *Phys. Rev. A* **105**, 023109 (2022).
- [22] C. Shah, H. Jörg, S. Bernitt, S. Dobrodey, R. Steinbrügge, C. Beilmann, P. Amaro, Z. Hu, S. Weber, S. Fritzsche, A. Surzhykov, J. R. Crespo López-Urrutia, and S. Tashenov, Polarization measurement of dielectronic recombination transitions in highly charged krypton ions, *Phys. Rev. A* **92**, 042702 (2015).
- [23] I. S. Gradshteyn and I. M. Ryzhik, *Table of Integrals, Series, and Products* (Academic Press, Cambridge, MA, 1980).
- [24] X.-M. Tong, L. Liu, and J.-M. Li, Relativistic effect of atomic radiative processes, *Phys. Rev. A* **49**, 4641 (1994).
- [25] U. Fano, Description of states in quantum mechanics by density matrix and operator techniques, *Rev. Mod. Phys.* **29**, 74 (1957).
- [26] V. V. Balashov, A. N. Grum-Grzhimailo, and N. M. Kabachnik, *Polarization and Correlation Phenomena in Atomic Collisions* (Springer, New York, 2000).
- [27] K. Blum, *Density Matrix Theory and Applications* (Springer, New York, 1981).
- [28] M. F. Gu, The flexible atomic code, *Can. J. Phys.* **86**, 675 (2008).
- [29] M. Vockert, G. Weber, H. Bräuning, A. Surzhykov, C. Brandau, S. Fritzsche, S. Geyer, S. Hagmann, S. Hess, C. Kozhuharov, R. Martin, N. Petridis, R. Hess, S. Trotsenko, Y. A. Litvinov, J. Glorius, A. Gumberidze, M. Steck, S. Litvinov, T. Gaßner *et al.*, Radiative electron capture as a tunable source of highly linearly polarized x rays, *Phys. Rev. A* **99**, 052702 (2019).
- [30] R. H. Pratt, R. D. Levee, R. L. Pexton, and W. Aron, Polarization correlations in atomic photoeffect, *Phys. Rev.* **134**, A916 (1964).
- [31] F. A. Parpia and A. K. Mohanty, Relativistic basis-set calculations for atoms with Fermi nuclei, *Phys. Rev. A* **46**, 3735 (1992).